Noncovalent Interactions

DOI: 10.1002/ange.201307500

Intramolecular Interactions of a Phenyl/Perfluorophenyl Pair in the Formation of Supramolecular Nanofibers and Hydrogels**

*Shu-Min Hsu, Yu-Chun Lin, Jui-Wen Chang, Yu-Hao Liu, and Hsin-Chieh Lin**

Abstract: *A new system for the incorporation of a phenyl/perfluorophenyl pair in the structure of a peptide hydrogelator was developed. The strategy is based on the idea that the integration of an end-capped perfluorophenyl group and a phenylalanine with a phenyl moiety in the side chain forms an intramolecular phenyl/perfluorophenyl pair, which can be used to promote the formation of the supramolecular nanofibers and hydrogels. This work illustrates the importance of structure-hydrogelation relationship and provides new insights into the design of self-assembly nanobiomaterials.*

Herein, we demonstrate the first example of intramolecular binding of a phenyl/perfluorophenyl pair for the formation of supramolecular hydrogels as a candidate for potential biomaterials. Supramolecular hydrogels, a gel state resulting from self-assembly of small molecules in water, has become a rapidly expanding field in soft biomaterials.[1] Nowadays, a peptide-based supramolecular hydrogel is one of the most attractive strategies for developing soft biomaterials because of the tunable composition and architecture.[2] There are three major categories of peptide hydrogels: peptide amphiphiles,[3] ionic complimentary peptides,[4] and low-molecular-weight hydrogels.[5–11] The smallest molecular unit of a supramolecular hydrogel is denoted as a hydrogelator. A low-molecular-weight hydrogelator minimizes the available functionality which can participate in intermolecular interactions, thus providing useful probes of the scope and limitations of the molecules which form supramolecular hydrogels. Recently, a number of applications based on low-molecular-weight supramolecular hydrogels have been explored, including tissue engineering,[5,6] drug delivery,[7] enzyme assay,[8] protein separation,[9] biosensing,[10] and wound healing.[11]

The supramolecular synthon, the phenyl/perfluorophenyl pair, has attracted considerable interest because this motif is widely used in designing structures for crystal engineering and for reaction control in solution.[12] The packing of hexafluorobenzene or benzene in the crystal is that of a herringbone structure,[13] whereas an equimolar mixture of hexafluorobenzene and benzene are stacked alternatively and parallel.[14] Also, experimental studies in the gas and liquid phases show that the molecular planes between arenes are close to parallel.[15,16] The computational studies reveal that the formation of alternating and parallel packing of a hexafluorobenzene/benzene pair is the result of an optimization of quadrupole–quadrupole, dispersion, and C–H···F–C interactions.[12,17] In addition to the dimeric structure of the two aromatic rings in the presence of water, a trimeric complex of hexafluorobenzene/water/benzene is also possible. An earlier computational study on the potential energy surface of this system suggests the presence of the water sandwiched between two aromatics exhibits larger binding energy than that of the dimer with water removed.[18] It is known that a supramolecular nanofiber in a low-molecular-weight hydrogel may demand a well-ordered spatial arrangement in the π-stacking direction.[6] Therefore, we believe that the lowest ground-state energy from the alternating packing of the dimer or the water-assisted trimeric structure would be useful in the structural design of low-molecular-weight hydrogelators.

From a microscopic view, a supramolecular hydrogel is constructed by physical crosslinks and entanglements of supramolecular nanofibers which are composed of self-assembled hydrogelators. An efficient way to construct a low-molecular-weight hydrogelator is to attach an π-conjugated system, such as fluorenylmethoxycarbonyl (Fmoc) or naphthyl (Nap), to the N terminus of a short peptide.[19] In this work, a new system incorporating the phenyl/perfluorophenyl pair in the structure of a hydrogelator has been developed. The strategy is based on the idea that the incorporation of a perfluorophenyl group as the end-capped π-conjugated part, and a linking amino acid of phenylalanine with a phenyl moiety in the side chain forms a new intramolecular building block, a phenyl/perfluorophenyl pair, for the efficient formation of supramolecular hydrogels (Scheme 1). Note that the use of intermolecular interactions for phenyl/perfluorophenyl pairs to promote the supramolecular hydrogelation have been demonstrated recently.[20] We stress that the presence of the intramolecular building block would facilitate the intermolecular self-assembly in terms of a low-energy alternate packing of phenyl/perfluorophenyl systems in the crystals.[14] As shown in Scheme 1, there are two possible routes to form self-assembled nanofibers. The proposed route 1 represents the alternating packing of the phenyl/perfluorophenyl pair as a result of a water-assisted effect induced by the quadrupole–dipole–quadrupole interactions.[18] The route 2 shows that the alternating arrangement of two aromatics is the consequence of the balance of

[*] S.-M. Hsu, Y.-C. Lin, J.-W. Chang, Y.-H. Liu, Prof. Dr. H.-C. Lin
Department of Materials Science and Engineering
National Chiao Tung University
Hsinchu, 300, Taiwan (Republic of China)
E-mail: hclin45@nctu.edu.tw

[**] We thank Prof. Shiaw-Guang Hu for technical support. We also thank the National Science Council of the Republic of China, Taiwan (Grant No. NSC 100-2113M-009-015-MY2) and the "Aim for the Top University" program of the National Chiao Tung University and Ministry of Education, Taiwan, R.O.C. for funding. We are also grateful to the National Center for High-performance Computing of Taiwan for computer time and facilities.

Supporting information for this article is available on the WWW under http://dx.doi.org/10.1002/anie.201307500.

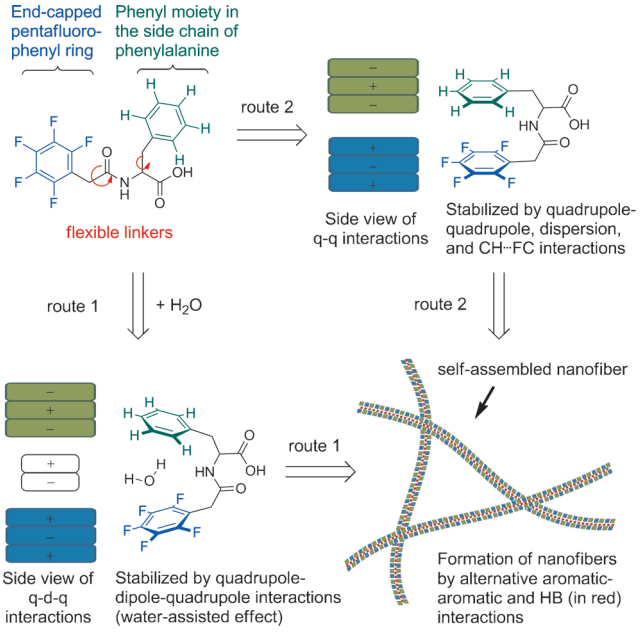

Scheme 1. The proposed routes for intramolecular interactions and intermolecular self-assembly of hydrogelators (q = quadrupole, d = dipole, HB = hydrogen bonding).

quadrupole–quadrupole, dispersion, and CH–FC interactions.[12,17] Both routes form the intramolecular alternative pair which may facilitate the formation of self-assembled nanofibers and hydrogels. A series of molecules (Scheme 2) were prepared and the following features are addressed herein: 1) determination of the peptide sequences that are valid for triggering molecular hydrogelation under neutral conditions for the development of soft biomaterials, 2) characterization of the intermolecular interactions and physical properties of gel materials, and 3) elucidation of the importance of intramolecular building blocks on self-assembly and hydrogelation.

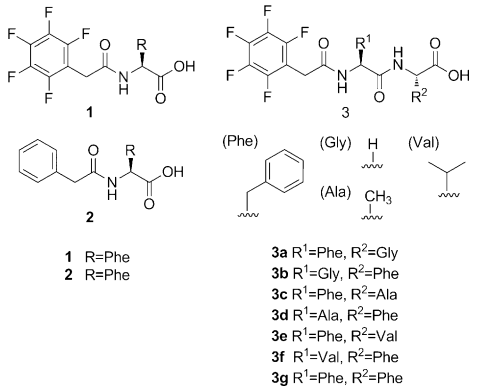

Scheme 2. The chemical structures of the compounds **1**–**3**.

All of the peptides (**1**–**3**) were synthesized by solid-phase peptide synthesis (SPPS, see the Supporting Information for details). The hydrogels of peptides were prepared by a sequential change in pH, and the resulting optical images were collected (insets of Figure 1). The microscopic nanostructures of the negatively stained hydrogels were measured by transmission electron microscopy (TEM; Figure 1). We found that dissolving the amino-acid derivative **1** at a concentration of 1 wt% with a pH of 5.0 in aqueous solution led to the formation of a hydrogel (Figure 1). The TEM analysis revealed that the hydrogel of **1** consisted of a fibrous network and these nanofibers entangle to trap water and result in a hydrogel. These observations indicate self-assembly and hydrogelation occurred in **1**. Alternatively, the analogue **2** in the concentration range of 1–3 wt% remains a clear solution. The dramatic change in the formation of the hydrogel for **1** compared with that of **2** illustrates the remarkable fluorous effect on self-assembly and hydrogelation. The formation of the hydrogel of **1** confirms that the direct attachment of a pentafluorobenzyl group (PFB) to the N terminus of the L-phenylalanine (L-Phe) is a valid approach for designing a new supramolecular hydrogelator. To examine the applicability of this newly discovered building block (PFB-L-Phe) for the design of peptide-based hydrogelators, we prepared seven PFB-capped molecules with various peptide sequences of L-Phe-L-Gly (**3a**), L-Gly-L-Phe (**3b**), L-Phe-L-Ala (**3c**), L-Ala-L-Phe (**3d**), L-Phe-L-Val (**3e**), L-Val-L-Phe (**3f**) and L-Phe-L-Phe (**3g**). The hydrogelation tests of **3a** (1 wt%), and **3b** (1–3 wt%) show that only **3a** formed a hydrogel, thus indicating that the presence of the building block of PFB-L-Phe is crucial. The different behavior between L-Phe-L-Gly and L-Gly-L-Phe in the Fmoc-capped hydrogelators has been described recently.[21] The molecular weights of **3a** and **3b** are essentially the same. The only difference between the two molecules is the position of the benzyl side chain of the amino acid, thus implying the importance of the intramolecular effect of the PFB-L-Phe building block of **3a** for the formation of the hydrogel, because the intermolecular interactions of phenyl and pentafluorophenyl groups between different molecules of **3b** do not trigger the formation of self-assembly

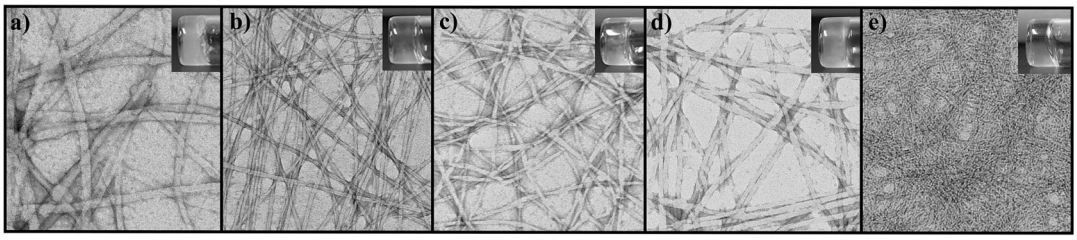

Figure 1. Optical and negatively stained TEM images of hydrogels for a) **1**, b) **3a**, c) **3c**, d) **3e**, and e) **3g** at a concentration of 1 wt% (scale bar = 50 nm).

Table 1: Physical properties of peptide-based hydrogelators and related compounds.

Entry	pH	Appearance[a]	Conc. (cgc)[b] [wt%]	$T_{gel\text{-}sol}$ [°C]	G′, G″ [Pa]	Fiber diameter [nm]
1	5.0	SG	1 (1.0)	56	3.0×10^3, 1.5×10^2	31 ± 5
2	5.0	TS	1–3			
3a	7.0	TG	1 (0.2)	48	1.2×10^4, 1.5×10^3	8 ± 1
3b	7.0	TS	1–3			
3c	6.0	TG	1 (0.2)	48	4.4×10^3, 3.0×10^2	10 ± 2
3d	6.0	TS	1–3			
3e	6.0	SG	1 (0.2)	46	3.2×10^3, 8.7×10^1	14 ± 2
3f	6.0	TS[c]	1–3			
3g	10.0	TG	1 (0.5)	45	3.4×10^4, 8.0×10^3	5 ± 1

[a] TG: transparent gel; SG: semitranslucent gel; TS: transparent solution. [b] cgc is the lower critical gelation concentration. [c] Transparent viscous solution.

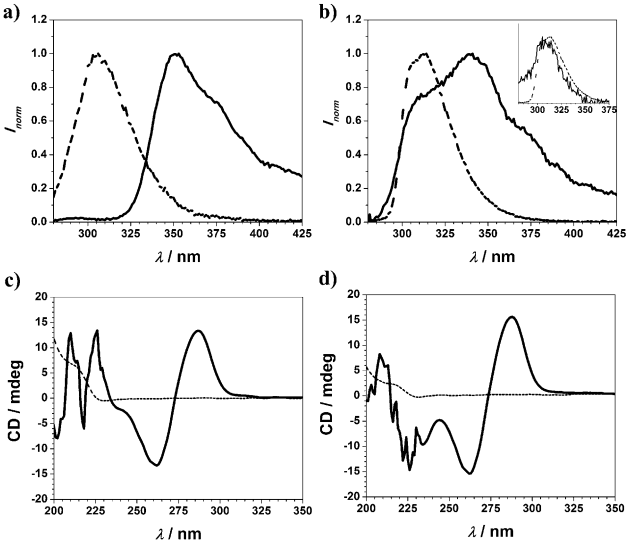

Figure 2. Normalized fluorescence emission spectra of a) **1** (pH 5), and b) **3a** (pH 7) in water. Solid line: 1 wt% (gel); dashed line: 0.01 wt% (solution). The inset of (b) is the emission spectra for **3a** (pH 7, dashed line) and **3b** (pH 7, solid line). CD spectra of the hydrogels of c) **1** (pH 5) and d) **3a** (pH 7) in water. Solid line: 1 wt% (gel); dashed line: 0.01 wt% (solution).

nanofibers. In addition to the dipeptide of **3a**, the dipeptides of **3c**, **3e**, and **3g** formed supramolecular hydrogels at a concentration of 1 wt% (Figure 1), thus showing the generality of the use of the PFB-L-Phe in the structural design of the peptide-based hydrogelators. The hydrogelation of the dipeptides were dependent on pH values (Table 1), which can be explained by the equilibrium between the carboxylic acid and carboxylate.[22] It is noteworthy that the hydrogelator **3a** formed a hydrogel under neutral conditions. The lower critical gel concentration (cgc) is 0.2 wt% for **3a**, **3c**, and **3e**, and 0.5 wt% for **3g**, thus indicating that the presence of hydrophobic and bulky side chains near the C terminus in **3g** would lead to a higher cgc. The statistical analysis of the TEM images of the dipeptides **3a**, **3c**, **3e**, and **3g** reveals that dipeptides form high-density and thinner fibrils in the hydrogels compared to those of **1** (Table 1). These results confirm that self-assembly nanofibers of **1**, **3a**, **3c**, **3e**, and **3g** act as the matrices to sustain the hydrogels.

While it remains a challenge to determine the accurate molecular arrangements of the hydrogelators in the gel state, the spectroscopic characterization of the hydrogels provides useful and relevant information regarding the interactions of the hydrogelators.[6,21] The fluorescence emission was used to monitor the environment of aromatic moieties of the hydrogelators to assess the aromatic–aromatic (π–π) interactions.[19b] The emission spectra of **1** and **3a** were obtained with an excitation wavelength of $\lambda = 260$ nm for aromatic rings under the gelation conditions (Figure 2a and b). In Figure 2a, a clear emission band at $\lambda = 308$ nm for **1** in dilute solution was observed. In the gel state, there appears to be a red shift in the emission (ca. 350 nm), thus indicating π–π interactions between aromatic rings occur in the gel state of **1**. The emission spectrum of the **3a** gel exhibited a red-shifted and broad peak in comparison with that of the dilute solution. This change in the emission profile originates from the intermolecular aromatic–aromatic interactions. In addition, the emission spectra of **3a** and **3b** in dilute solutions are shown in the inset of Figure 2b. The red shift for the emission of **3a** relative to **3b** is essential. This difference is likely a result of a stronger intramolecular aromatic–aromatic interactions for the phenyl/pentafluorophenyl pair in **3a** (see the Supporting Information for **3c**, **3e**, and **3f**).[23] Circular dichroism (CD) was used to explore the superstructures of these self-assembled hydrogels. In Figures 2c and d, both the CD spectra of the hydrogels of **1** and **3a** revealed bisignated Cotton effects, with a negative part at $\lambda =$ 261 nm and a positive part at $\lambda = 287$ nm. According to the exciton-coupling model,[24] a bisignated Cotton effect is consistent with the interacting π-conjugated systems in an ordered arrangement.[25] CD spectra of the hydrogels **3c** and **3g** showed similar bisignated Cotton effects, while by increasing the bulkiness of the aliphatic side chain of the amino acid, such with as **3e**, there are fewer modes of aromatic–aromatic interactions ($\lambda = 260$–330 nm) between phenyl and pentafluorophenyl rings (see the Supporting Information for details). Furthermore, the CD spectrum is also a useful tool to study the formation of the extended hydrogen-bonding interactions such as in β-sheet or β-turn structures.[19b] Except for the hydrogel of **1**, the dipeptide hydrogels of **3a**, **3c**, **3e**, and **3g** revealed few negative peaks in the range of $\lambda = 215$–240 nm, thus implying the possibility of the formation of β-sheet and/or β-turn structures.[19b] To confirm this, FT-IR was employed for the analysis of the secondary structures of the self-assembly nanostructures in hydrogels.[6,21] FT-IR spectrum of the hydrogel of **1** revealed that there is no secondary structure formed in the hydrogel, thus suggesting the flexibility of the hydrogelator **1** does not allow the single amino acid to interlock in a β-sheet conformation (see Figure S7 in the Supporting Information). On the contrary, the spectra of **3a**, **3c**, **3e**, and **3g** gels showed two intense peaks located around 1656 cm^{-1} and 1630 cm^{-1}, as

well as a less intense peak around 1545 cm^{-1}, which is the typical characteristic of extended β-sheet absorptions.[26] As suggested by the spectroscopic data, the formation of extended self-assembled nanostructures occurs under the gelation conditions for **1**, thus indicating that the aromatic–aromatic interactions may be the major driving force behind the self-assembly of the hydrogelators. Although we do not observe extended hydrogen-bonding interactions for the hydrogel of **1**, a peak for the molecular dimer was found in the mass spectrum.[27] This observation can be reasonably explained by the hydrogen-bonding interactions of two carboxy end groups.[28] According to the spectroscopic characterizations of the dipeptide hydrogels of **3a**, **3c**, **3e** and **3g**, the cooperative effect of aromatic–aromatic and hydrogen-bonding interactions might constitute the main driving force for the formation of the self-assembled nanofibers and hydrogels. Based on the spectroscopic data of **3a**, we have built a molecular packing model which can fulfill the requirements of extended aromatic–aromatic interactions, extended hydrogen-bonding interactions, and the intramolecular alternative packing of phenyl and perfluorophenyl rings (see Figure S8).

It is noteworthy that the hydrogelator **1** has the minimum number of atoms (38 atoms) in an acyclic amino-acid-based hydrogelator to date.[29] Based on the hydrogelation tests, TEM images, and spectroscopic data, the experimental results are quite consistent with our hypothesis of the formation of an intramolecular building block. However, the exact nature of the formation of nanofibers in aqueous solution is still debatable, despite the well-documented preference of the intramolecular alternating arrangement of the two aromatic rings in **1**. To prove this, we employed a ^{1}H-^{19}F HOESY technique which has great utility in structural and conformational analysis of organic molecules in solution. This experiment measures the distance-dependent nuclear Overhauser effect between nonbonded nuclei separated by less than 0.5 nm.[30] Owing to these advantages, the ^{1}H-^{19}F HOESY experiment was used to investigate the conformation of **1** in D_2O.[31] In the ^{19}F NMR spectrum (Figure 3a), the appearance of three peaks at $\delta = -145.2$, -166.4, and -159.8 ppm were assigned to the *ortho*, *meta*, and *para* fluorine atoms, respectively, of the pentafluorophenyl group.[32] The intramolecular correlations of two aromatic rings in **1** can be discerned in a ^{1}H-^{19}F HOESY spectrum displaying cross-correlations between the ^{19}F signals of the pentafluorophenyl group and ^{1}H signals of phenyl ring in phenylalanine. As shown in Figure 3b, these correlations between the *ortho*-fluorine atoms ($\delta = -145.2$ ppm in the ^{19}F NMR spectrum) of the pentafluorophenyl group and hydrogen atoms ($\delta =$ 7.2 ppm in the ^{1}H NMR spectrum) on the phenyl side chain of phenylalanine were detected as crosspeaks in the ^{1}H-^{19}F HOESY experiment, thus implying that two aromatic rings are situated in close proximity in **1**.

To gather more insight into the geometry of **1**, quantum-chemical calculations were performed on **1** to explore whether the water-assisted effect is possible in the ground state of **1**. The Moller-Plesset (MP2) perturbation theory with a 6-31G** basis set was used to calculate the geometries and energies for **1** with (**1-A**) and without (**1-B**) the sandwiched

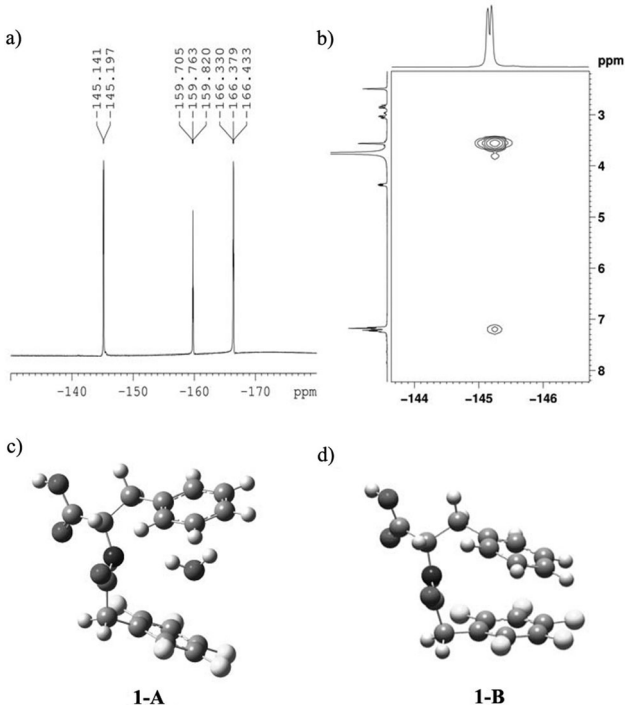

Figure 3. Experimental a) ^{19}F NMR and b) ^{1}H-^{19}F HOESY spectra of **1** dissolved in D_2O.[31] Optimized geometries of c) **1-A** and d) **1-B** calculated at the MP2 at 6-31G** level of theory.

water (Figure 3).[33] This method has been used extensively in the studies of perfluoroarene/arene pairs, and has given reliable results when compared to experimental data and other highly extensive ab initio calculations.[33c] Recently, a concerted effort on the experimental and theoretical studies reveal that the dipole–quadrupole interactions between water and the perfluorobenzene ring are essential.[34] An earlier computational study on the potential energy surface of perfluorobenzene/benzene systems suggests that the presence of water sandwiched between two aromatics results in larger binding energy compared with that of the aromatic dimer.[18] A plausible reason for the formation of the trimeric structure is that the benzene and perfluorobenzene rings can serve as a proton acceptor and a lone pair acceptor, respectively. The MP2 optimized geometries of **1-A** and **1-B** are shown in Figures 3c and d, respectively. Both of them show the tilted structures, and the higher stabilities of tilted structures compared with parallel ones can be ascribed to the structural flexibility and the attractive electrostatic interactions between the oppositely charged peripheries of the phenyl and pentafluorophenyl rings.[18] The distances between the two arenes in **1-A** and **1-B** are listed in the Supporting Information. The MP2 calculations of water–hydrogelator interactions were a posteriori corrected by a standard counterpoise (CP) procedure.[18,33c] The difference in total energies between **1-A** and **1-B** + H_2O is -4.3 kcal mol^{-1}, thus indicating that the presence of the water sandwiched between the arenes stabilizes the ground-state energy of **1-A**. Based on the computational data, the sandwiched water in **1** may play a pivotal role in accommodating an appropriate geometry which facilitates the self-assembly and hydrogelation. The

optimized geometry of **1-B** reveals that all of fluorine atoms should appear as crosspeaks in ^{1}H-^{19}F HOESY (see the Supporting Information for details). However, there is no crosspeak from the *meta*- or *para*-fluorine atoms in the ^{1}H-^{19}F HOESY spectrum of **1**. This result can be explained by the structure of **1-A**. In the presence of the sandwiched water, only the fluorine atom at the *ortho* position correlates the hydrogen atoms of the phenyl ring because the distances of these atoms are less than 0.5 nm. Based on energy and geometry considerations, the water-assisted effect originating from dipole–quadrupole interactions between water and the phenyl/perfluorophenyl pair might play a crucial role in the formation of the supramolecular hydrogel of **1**. The molecules **3a**, **3c**, **3e**, and **3g** behave similarly and the results are collected in the Supporting Information. According to the experimental and computational results, route 1 in Scheme 1 might be the plausible pathway to trigger the self-assembly in the system.

Supramolecular hydrogels are potentially useful scaffolds for the application in tissue engineering.[6] In terms of a hydrogel as three-dimensional (3D) environment for cell growth, the following criteria should be reached: 1) the gel-to-sol transition temperature ($T_{gel\text{-}sol}$) of the hydrogel is higher than body temperature, 2) the mechanical properties of the hydrogel support the mass of a cell, and 3) the hydrogel is biocompatible with no inhibitory effect on cell-matrix interactions. In general, because live cells are usually cultured at body temperature, the $T_{gel\text{-}sol}$ of a 3D culture medium needs to be higher than the physiologically relevant temperature (i.e., 37 °C, body temperature). As shown in Table 1, all gel-to-sol transition temperatures of hydrogels of **1**, **3a**, **3c**, **3e**, and **3g** are higher than 37 °C, thus pointing to potential uses of these hydrogels as scaffolds for tissue engineering. The mechanical property of a hydrogel can be assessed by oscillatory rheology. This method provides two essential parameters for hydrogels. They are the elastic and viscous responses which are denoted as storage modulus (G′) and loss modulus (G″), respectively. While the ideal storage modulus varies depending on cell type, a minimum storage modulus of around 100 Pa is necessary to support the mass of a cell.[35–37] In comparison with various hydrogels, the viscoelastic properties of all hydrogels are determined at the concentration of 1 wt.% and the data are collected in Table 1. In Figure 4a, the storage moduli of hydrogels of **1** and **3a** (see the Supporting Information for **3c**, **3e**, and **3g**) are found to be higher than their loss moduli, thus indicating these hydrogels are stable elastic materials rather than viscous ones. The storage modulus of hydrogel **1** is 3 KPa which is sufficient to support the mass of a cell. The storage moduli of dipeptides are collected in Table 1, and the hydrogel of **3g** exhibits the highest storage modulus (34 KPa) among the dipeptides, thus implying that the relatively thinner nanofibers (5 nm) cause more significant physical crosslinks and entanglements in the system.

Hydrogels of **1** and dipeptide **3a** (hydrogelation in neutral condition) were subsequently tested for their ability to support the biocompatibilities of CTX TNA2 cells. The biocompatibilities of **1** and **3a** were examined using a colorimetric assay with 3-(4,5-dimethylthiazol-2-yl)-2,5-diphenyltetrazolium bromide (MTT). The experiments (Figures 4b and c) reveal that after being incubated with the hydrogelators **1** and **3a** in a concentration range of (10–500 μM) for 48 hours, cells that were grown in liquid medium showed the proliferation capacities with high viability. The survival ratio of **1** and **3a** were above 80% at 500 μM, and their morphologies were similar to the control cells that were grown in the medium without hydrogelators. The concentrations of **1** and **3a** required for 50% inhibition (IC_{50}) are higher than 500 μM, thus indicating that the hydrogelators are biocompatible.[12b] Furthermore, we also used a wound-healing assay[38] to examine the capability of the hydrogels of **3a** where the cell/matrix interactions are held (see Figure S10). The presence of **3a** in the cell culture shows little inhibitory effect on the migration of the CTX TNA2 cells as compared with that of the reference, which further supports the biocompatibility of **3a**.

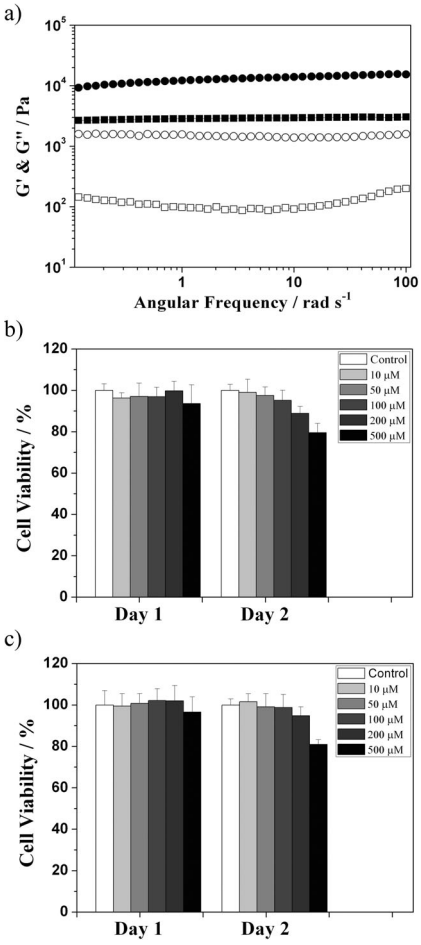

Figure 4. a) The frequency sweep of the supramolecular hydrogels of **1** and **3a** at a concentration of 1 wt%. G′ of **1** (closed square) and **3a** (closed circle); G″ of **1** (open square) and **3a** (open circle). Viability of CTX TNA2 cells incubated with 10, 50, 100, 200, and 500 μM of b) **1** and c) **3a** after 24 and 48 h.

In summary, we have detailed a new series of low-molecular-weight hydrogelators and proved that the intramolecular alternative packing of the phenyl/perfluorophenyl pair can be used to promote the formation of the supra-

molecular hydrogels. According to experimental and computational results, the presence of the water sandwiched between the aromatic rings may assist in the formation of an intramolecular phenyl/perfluorophenyl complex. It is noteworthy that the amino-acid derivative **1** has the minimum number of atoms in an acyclic amino-acid-based hydrogelator prepared to date, and this minimal self-assembled scaffold can fundamentally achieve all the hydrogel features associated with larger peptides. Additionally, the PFB dipeptides were also identified. Based on the spectroscopic data, the formation of extended self-assembled nanostructures occurs at the gelation conditions of dipeptide hydrogelators, thus indicating that the aromatic–aromatic and hydrogen-bonding interactions may be the major driving force behind the self-assembly of the hydrogelators. The structural and physical properties of dipeptide hydrogels were found to be dictated by the amino-acid sequence of the peptide building blocks. The biocompatibility tests of the hydrogels indicate the newly discovered hydrogelators are potential biomaterials. This work illustrates the importance of structure–hydrogelation relationship and provides new insights into the design of self-assembled nanobiomaterials.

Please note: Minor changes have been made to this manuscript since its publication in *Angewandte Chemie* Early View. The Editor.

Received: August 26, 2013
Revised: October 17, 2013
Published online: January 13, 2014

Keywords: hydrogels · nanofibers · noncovalent interactions · self-assembly · supramolecular chemistry

[1] H.-C. Lin, B. Xu, *Applications of Supramolecular Chemistry* (Eds.: H.-J. Schneider), CRC, Boca Raton, FL, **2012**, chap. 13.
[2] J. B. Matson, S. I. Stupp, *Chem. Commun.* **2012**, *48*, 26 – 33.
[3] a) J. D. Hartgerink, E. Beniash, S. I. Stupp, *Science* **2001**, *294*, 1684 – 1688; b) G. A. Silva, C. Czeisler, K. L. Niece, E. Beniash, D. A. Harrington, J. A. Kessler, S. I. Stupp, *Science* **2004**, *303*, 1352 – 1355.
[4] a) S. Zhang, *Acc. Chem. Res.* **2012**, *45*, 2142 – 2150; b) Z. Luo, S. Zhang, *Chem. Soc. Rev.* **2012**, *41*, 4736 – 4754.
[5] a) A. Mahler, M. Reches, M. Rechter, S. Cohen, E. Gazit, *Adv. Mater.* **2006**, *18*, 1365 – 1370; b) T. C. Holmes, S. de Lacalle, X. Su, G. S. Liu, A. Rich, S. G. Zhang, *Proc. Natl. Acad. Sci. USA* **2000**, *97*, 6728 – 6733; c) L. A. Haines, K. Rajagopal, B. Ozbas, D. A. Salick, D. J. Pochan, J. P. Schneider, *J. Am. Chem. Soc.* **2005**, *127*, 17025 – 17029; d) K. M. Galler, L. Aulisa, K. R. Regan, R. N. D'Souza, J. D. Hartgerink, *J. Am. Chem. Soc.* **2010**, *132*, 3217 – 3223.
[6] A. M. Smith, R. J. Williams, C. Tang, P. Coppo, R. F. Collins, M. L. Turner, A. Saiani, R. V. Ulijn, *Adv. Mater.* **2008**, *20*, 37 – 41.
[7] a) J. Li, Y. Kuang, Y. Gao, X. Du, J. Shi, B. Xu, *J. Am. Chem. Soc.* **2013**, *135*, 542 – 545; b) H. Wang, J. Wei, C. Yang, H. Zhao, D. Li, Z. Yin, Z. Yang, *Biomaterials* **2012**, *33*, 5848 – 5853; c) X. Li, Y. Kuang, J. Shi, Y. Gao, H.-C. Lin, B. Xu, *J. Am. Chem. Soc.* **2011**, *133*, 17513 – 17518; d) H. Komatsu, S. Matsumoto, S. Tamaru, K. Kaneko, M. Ikeda, I. Hamachi, *J. Am. Chem. Soc.* **2009**, *131*, 5580 – 5585; e) J. Boekhoven, M. Koot, T. A. Wezendonk, R. Eelkema, J. H. van Esch, *J. Am. Chem. Soc.* **2012**, *134*, 542 – 545; f) F. Zhao, M. L. Ma, B. Xu, *Chem. Soc. Rev.* **2009**, *38*, 883 – 891.
[8] a) S. Kiyonaka, K. Sada, I. Yoshimura, S. Shinkai, N. Kato, I. Hamachi, *Nat. Mater.* **2004**, *3*, 58 – 64; b) Z. Yang, G. Liang, B. Xu, *Acc. Chem. Res.* **2008**, *41*, 315 – 326; c) Z. Yang, K. Xu, Z. Guo, Z. Guo, B. Xu, *Adv. Mater.* **2007**, *19*, 3152 – 3156.
[9] Y. Gao, M. J. C. Long, J. F. Shi, L. Hedstrom, B. Xu, *Chem. Commun.* **2012**, *48*, 8404 – 8406.
[10] a) A. Wada, S. Tamaru, M. Ikeda, I. Hamachi, *J. Am. Chem. Soc.* **2009**, *131*, 5321 – 5330; b) A. Rajagopalan, W. Kroutil, *Mater. Today* **2011**, *14*, 144 – 152; c) S. C. Bremmer, J. Chen, A. J. McNeil, M. B. Soellner, *Chem. Commun.* **2012**, *48*, 5482 – 5484.
[11] a) Z. Yang, G. Liang, M. Ma, A. S. Abbah, W. W. Lu, B. Xu, *Chem. Commun.* **2007**, 843 – 845; b) X. Li, Y. Kuang, H.-C. Lin, Y. Gao, J. Shi, B. Xu, *Angew. Chem.* **2011**, *123*, 9537 – 9541; *Angew. Chem. Int. Ed.* **2011**, *50*, 9365 – 9369.
[12] a) L. M. Salonen, M. Ellermann, F. Diederich, *Angew. Chem.* **2011**, *123*, 4908 – 4944; *Angew. Chem. Int. Ed.* **2011**, *50*, 4808 – 4842; b) K. Reichenbächer, H. I. Süss, J. Hulliger, *Chem. Soc. Rev.* **2005**, *34*, 22 – 30.
[13] a) E. G. Cox, D. W. J. Cruickshank, J. A. S. Smith, *Proc. R. Soc. London Ser. A* **1958**, *247*, 1 – 21; b) N. Boden, P. P. Davis, C. H. Stam, G. A. Wesselink, *Mol. Phys.* **1968**, *25*, 81 – 86.
[14] J. H. Williams, J. K. Cockcroft, A. N. Fitch, *Angew. Chem.* **1992**, *104*, 1666 – 1669; *Angew. Chem. Int. Ed. Engl.* **1992**, *31*, 1655 – 1657.
[15] J. M. Steed, T. A. Dixon, W. Klemperer, *J. Chem. Phys.* **1979**, *70*, 4940 – 4944.
[16] E. Bartsch, H. Bertagnolli, P. Chieux, *Ber. Bunsen-Ges.* **1986**, *90*, 34 – 46.
[17] E. A. Meyer, R. K. Castellano, F. Diederich, *Angew. Chem.* **2003**, *115*, 1244 – 1287; *Angew. Chem. Int. Ed.* **2003**, *42*, 1210 – 1250.
[18] M. Raimondi, G. Calderoni, A. Famulari, L. Raimondi, F. Cozzi, *J. Phys. Chem. A* **2003**, *107*, 772 – 774.
[19] a) D. M. Ryan, B. L. Nilsson, *Polym. Chem.* **2012**, *3*, 18 – 33; b) M. Ma, Y. Kuang, Y. Gao, Y. Zhang, P. Gao, B. Xu, *J. Am. Chem. Soc.* **2010**, *132*, 2719 – 2728.
[20] D. M. Ryan, T. M. Doran, B. L. Nilsson, *Langmuir* **2011**, *27*, 11145 – 11156.
[21] C. Tang, R. V. Ulijn, A. Saiani, *Langmuir* **2011**, *27*, 14438 – 14449.
[22] C. Tang, A. M. Smith, R. F. Collins, R. V. Ulijn, A. Saiani, *Langmuir* **2009**, *25*, 9447 – 9453.
[23] M.-Y. Yeh, H.-C. Lin, S.-L. Lee, C.-h. Chen, T.-S. Lim, W.-S. Fann, T.-Y. Luh, *Chem. Commun.* **2007**, 3459 – 3461.
[24] N. Harada, K. Nakanishi, *Circular Dichroic Spectroscopy. Exciton Coupling in Organic Stereochemistry*, University Science Books, Mill Valley, CA, **1983**.
[25] S. J. George, R. de Bruijn, Ž. Tomović, B. Van Averbeke, D. Beljonne, R. Lazzaroni, A. Schenning, E. W. Meijer, *J. Am. Chem. Soc.* **2012**, *134*, 17789 – 17796.
[26] a) E. Goormaghtigh, J. M. Ruysschaert, V. Raussens, *Biophys. J.* **2006**, *90*, 2946 – 2957; b) J. L. R. Arrondo, F. M. Goni, *Prog. Biophys. Mol. Biol.* **1999**, *72*, 367 – 405; c) A. Adochitei, G. Drochioiu, *Rev. Roum. Chim.* **2011**, *56*, 783 – 791; d) J. Kong, S. Yu, *Acta Biochim. Biophys. Sin.* **2007**, *39*, 549 – 559.
[27] A peak of the molecular dimer of **1** was found in the mass spectrum: MS [ESI$^-$]: calcd. 746.14, obsvd. 745.10 $[M-H]^-$.
[28] V. R. Thalladi, M. Nüsse, R. Boese, *J. Am. Chem. Soc.* **2000**, *122*, 9227 – 9236.
[29] J. Shi, Y. Gao, Z. Yang, B. Xu, *Beilstein J. Org. Chem.* **2011**, *7*, 167 – 172.
[30] K. Kawahara, N. Nemoto, D. Motooka, Y. Nishi, M. Doi, S. Uchiyama, T. Nakazawa, Y. Nishiuchi, T. Yoshida, T. Ohkubo, Y. Kobayashi, *J. Phys. Chem. B* **2012**, *116*, 6908 – 6915.
[31] For the solubility issue, we added about 5% $[D_6]$DMSO to the solution.
[32] a) H. Zheng, J. Gao, *Angew. Chem.* **2010**, *122*, 8817 – 8821; *Angew. Chem. Int. Ed.* **2010**, *49*, 8635 – 8639; b) G. W. Coates, A. R. Dunn, L. M. Henling, D. A. Dougherty, R. H. Grubbs,

Angew. Chem. **1997**, *109*, 290 – 293; *Angew. Chem. Int. Ed. Engl.* **1997**, *36*, 248 – 251.

[33] a) J. Hernández-Trujillo, F. Colmenares, G. Cuevas, M. Costas, *Chem. Phys. Lett.* **1997**, *265*, 503 – 507; b) A. P. West, Jr., S. Mecozzi, D. A. Dougherty, *J. Phys. Org. Chem.* **1997**, *10*, 347 – 350; c) S. Tsuzuki, T. Uchimaru, M. Mikami, *J. Phys. Chem. A* **2006**, *110*, 2027 – 2033.

[34] J. C. Amicangelo, D. G. Irwin, C. J. Lee, N. C. Romano, N. L. Saxton, *J. Phys. Chem. A* **2013**, *117*, 1336 – 1350.

[35] R. A. Hule, R. P. Nagarkar, A. Altunbas, H. R. Ramay, M. C. Branco, J. P. Schneider, D. J. Pochan, *Faraday Discuss.* **2007**, *139*, 251 – 264.

[36] L. Haines-Butterick, K. Rajagopal, M. Branco, D. Salick, R. Rughani, M. Pilarz, M. S. Lamm, D. J. Pochan, J. P. Schneider, *Proc. Natl. Acad. Sci. USA* **2007**, *104*, 7791 – 7796.

[37] C. Yan, D. Pochan, *Chem. Soc. Rev.* **2010**, *39*, 3528 – 3540.

[38] L. G. W. Rodriguez, J. L. Guan in *Cell Migration: Developmental Methods and Protocols*, *Vol. 294* (Ed.: J. L. Guan), Humana Press, Totowa, NJ, **2004**, p. 23.